JCB Article

Defective angiogenesis and fatal embryonic hemorrhage in mice lacking core 1–derived O-glycans

Lijun Xia,[1] Tongzhong Ju,[2] Andrew Westmuckett,[1] Guangyu An,[1] Lacramioara Ivanciu,[1] J. Michael McDaniel,[1] Florea Lupu,[1] Richard D. Cummings,[2,3] and Rodger P. McEver[1,2,3]

[1]Cardiovascular Biology Research Program, Oklahoma Medical Research Foundation, [2]Department of Biochemistry and Molecular Biology, and [3]Oklahoma Center for Medical Glycobiology, University of Oklahoma Health Sciences Center, Oklahoma City, OK 73104

The core 1 β1-3-galactosyltransferase (T-synthase) transfers Gal from UDP-Gal to GalNAcα1-Ser/Thr (Tn antigen) to form the core 1 O-glycan Galβ1-3GalNAcα1-Ser/Thr (T antigen). The T antigen is a precursor for extended and branched O-glycans of largely unknown function. We found that wild-type mice expressed the NeuAcα2-3Galβ1-3GalNAcα1-Ser/Thr primarily in endothelial, hematopoietic, and epithelial cells during development. Gene-targeted mice lacking T-synthase instead expressed the nonsialylated Tn antigen in these cells and developed brain hemorrhage that was uniformly fatal by embryonic day 14. T-synthase–deficient brains formed a chaotic microvascular network with distorted capillary lumens and defective association of endothelial cells with pericytes and extracellular matrix. These data reveal an unexpected requirement for core 1–derived O-glycans during angiogenesis.

Introduction

O-glycans containing GalNAc in α1 linkage to serines or threonines occur on many membrane and secreted proteins, particularly on mucins (Van den Steen et al., 1998). These types of O-glycans have a limited number of core structures. The most common structure is the core 1 disaccharide, which is also the precursor for the branched core 2 trisaccharide (Fig. 1 A). Both core 1 and core 2 structures can be further extended and modified into a diverse array of O-glycans of mostly unknown function. Some complex core 2 and extended core 1 O-glycans are components of mucin glycoprotein ligands for the selectins, which initiate leukocyte adhesion to vascular surfaces during infection, tissue injury, and immune surveillance (Fukuda, 2002; McEver, 2002; Van Zante and Rosen, 2003). Other core 1 or core 2 O-glycans may limit cell adhesion or modulate T cell function (Daniels et al., 2001; Moody et al., 2001, 2003; Fukuda, 2002).

The enzyme core 1 β1-3-galactosyltransferase (T-synthase) transfers Gal from UDP-Gal to GalNAcα1-Ser/Thr (Tn antigen) to form the core 1 O-glycan, Galβ1-3GalNAcα1-Ser/Thr (T antigen; Ju et al., 2002a,b). Many carcinomas express the unsubstituted T or Tn antigens (Brockhausen, 1999), and pathological exposure of the Tn antigen on cell surface or secreted proteins may cause autoimmune disease (Berger, 1999). Biochemical evidence and database searches suggest that a single gene, here termed *T-syn*, encodes all T-synthase activity (Ju et al., 2002a,b). Although it was proposed that another gene encodes a second T-synthase (Kudo et al., 2002), this gene actually encodes the chaperone protein Cosmc, which is required for folding and activity of the *T-syn*–encoded T-synthase (Ju and Cummings, 2002). To reveal the functions of core 1–derived O-glycans in vivo, we disrupted *T-syn* in mice.

Results

Disruption of *T-syn* causes fatal embryonic hemorrhage

Cre/loxP-mediated gene targeting was used to delete *T-syn* (Fig. 1, B–D). *T-syn*$^{+/-}$ mice developed normally. Matings between *T-syn*$^{+/-}$ mice generated 364 viable progeny, of which 175 (48%) were male and 189 (52%) were female.

The online version of this article contains supplemental material.

Address correspondence to Lijun Xia or Rodger P. McEver, Cardiovascular Biology Research Program, Oklahoma Medical Research Foundation, 825 N.E. 13th St., Oklahoma City, OK 73104. Tel.: (405) 271-6480. Fax: (405) 271-3137. email: lijun-xia@omrf.ouhsc.edu; rodger-mcever@omrf.ouhsc.edu

Key words: T-synthase; endothelial cell; galactosyltransferase; mucin; development

Abbreviations used in this paper: HPA, *Helix pomatia* agglutinin; MAG, myelin-associated glycoprotein; PNA, *Arachis hypogaea* agglutinin; sialyl-T antigen, NeuAcα2-3Galβ1-3GalNAcα1-Ser/Thr; sialyl-Tn antigen, NeuAcα2-6GalNAcα1-Ser/Thr; T antigen, Galβ1-3GalNAcα1-Ser/Thr; Tn antigen, GalNAcα1-Ser/Thr; T-synthase, core 1 β1-3-galactosyltransferase.

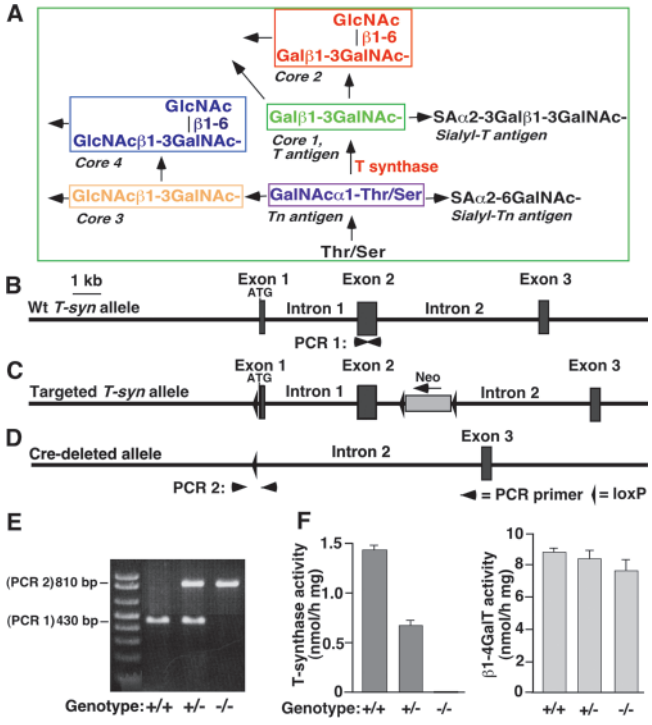

Figure 1. **Generation of T-synthase–deficient mice.** (A) Schematic of biosynthesis of the four common O-glycan core structures. The cores can be further extended and modified as indicated by additional arrows. The biosynthetic step that T-synthase catalyzes is shown. (B) Wild-type (Wt) *T-syn* allele showing the site of PCR 1 used for genotyping. (C) Targeted *T-syn* allele in embryonic stem cells after homologous recombination with the targeting vector. Exons 1 and 2 and a neomycin cassette (*Neo*) are flanked by three loxP sites. (D) Deletion of loxP-flanked exons 1 and 2 and Neo in embryonic stem cells after in vitro Cre-mediated recombination. The site of PCR 2 used for genotyping is indicated. (E) PCR genotyping of DNA from mouse embryos. PCR 1 amplifies a 430-bp fragment from the Wt allele, and PCR 2 amplifies an 810-bp fragment from the Cre-deleted allele. (F) T-synthase and β1-4-galactosyltransferase (β1-4GalT) activities in E12 tissue extracts. The data represent the mean ± SD of three independent measurements.

Genotyping identified 136 (37%) *T-syn*$^{+/+}$ progeny and 228 (63%) *T-syn*$^{+/-}$ progeny but did not identify *T-syn*$^{-/-}$ progeny. To determine whether deletion of *T-syn* on both alleles caused embryonic lethality, we analyzed 293 embryos at embryonic days 9–16 (E9–16) from timed matings of *T-syn*$^{+/-}$ mice. Genotyping revealed 78 (27%) *T-syn*$^{+/+}$, 142 (48%) *T-syn*$^{+/-}$, and 73 (25%) *T-syn*$^{-/-}$ progeny (Fig. 1 E). T-synthase activity in tissue extracts was reduced ~50% in E12 *T-syn*$^{+/-}$ embryos and was eliminated in *T-syn*$^{-/-}$ embryos, whereas the activity of β1-4-galactosyltransferase, which transfers Gal from UDP-Gal to GlcNAcβ1-R, was similar in embryos of all genotypes (Fig. 1 F). This result confirms that *T-syn* encodes all T-synthase activity, at least through this stage of development. This distinguishes *T-syn* from typical multigene families of glycosyltransferases that encode several enzymes with related structures and functions (Lowe and Marth, 2003).

At E9 *T-syn*$^{-/-}$ embryos appeared developmentally normal but thereafter, they developed progressively larger hemorrhages in the brain and spinal cord, with secondary bleeding into the ventricles and spinal canal (Fig. 2). Anemia was frequent, but only after bleeding occurred, and was associated with growth retardation but not with obvious defects in organogenesis. Histological examination revealed no placental abnormalities (unpublished data). Embryonic hemorrhage invariably preceded death, supporting a casual relationship. All *T-syn*$^{-/-}$ embryos died by E14, virtually always at E13 or E14.

T-syn$^{-/-}$ embryos express the Tn antigen but not the T antigen

To determine whether the levels of T-synthase activity affected core 1 O-glycosylation in vivo, we probed blots of embryonic extracts with *Arachis hypogaea* agglutinin (PNA), a lectin that recognizes the nonsialylated T antigen, and with *Helix pomatia* agglutinin (HPA), a lectin that recognizes the nonsialylated Tn antigen (Fig. 3 A). PNA bound to many glycoproteins from *T-syn*$^{+/+}$ and *T-syn*$^{+/-}$ embryos but not from *T-syn*$^{-/-}$ embryos. HPA bound to many glycoproteins from *T-syn*$^{-/-}$ embryos but exhibited little or no binding to glycoproteins from *T-syn*$^{+/+}$ and *T-syn*$^{+/-}$ embryos. Enzymatic desialylation of glycoproteins from *T-syn*$^{+/+}$ and *T-syn*$^{+/-}$ embryos was required to expose binding sites for PNA, indicating that sialic acid capped most core 1 O-glycans to form the NeuAcα2-3Galβ1-3GalNAcα1-Ser/Thr (sialyl-T antigen; Fig. 1 A). In contrast, desialylation of glycoproteins from *T-syn*$^{-/-}$ embryos was not required to expose binding sites for HPA, suggesting that sialic acid did not cap most of the Tn antigen to form the NeuAcα2-6GalNAcα1-Ser/Thr (sialyl-Tn antigen; Fig. 1 A).

To determine which cells expressed core 1 O-glycans in vivo, we probed embryonic tissue sections with mAbs to the T antigen, Tn antigen, or sialyl-Tn antigen. Anti-T stained endothelial, hematopoietic, and epithelial cells in tissues of *T-syn*$^{+/+}$ embryos, but only after enzymatic desialylation of the tissue sections (Fig. 3, C and D, and not depicted). In contrast, anti-Tn stained endothelial, hematopoietic, and epithelial cells in tissues of *T-syn*$^{-/-}$ embryos (Fig. 3 E). Enzymatic desialylation of tissue sections did not enhance binding of anti-Tn to *T-syn*$^{-/-}$ embryos (unpublished data). Furthermore, anti–sialyl-Tn did not stain *T-syn*$^{-/-}$ embryos (Fig. 3 F), although it did stain fixed Jurkat cells, which are known to express the sialyl-Tn antigen (unpublished data). Anti-T did not stain *T-syn*$^{-/-}$ embryos, and anti-Tn did not stain *T-syn*$^{+/+}$ embryos (Fig. 3 B). These results corroborate the lectin blotting data, and they demonstrate that sialic acid modifies the T antigen on *T-syn*$^{+/+}$ embryos but does not appreciably modify the Tn antigen on *T-syn*$^{-/-}$ embryos. Epithelial cells in some adult tissues transfer GlcNAc from UDP-GlcNAc to the Tn antigen to form the core 3 disaccharide, which is also the precursor for core 4 O-glycans (Van den Steen et al., 1998; Brockhausen, 1999; Fig. 1 A). However, Fig. 3 E demonstrates that *T-syn*$^{-/-}$ embryos do not synthesize sufficient core 3 O-glycans to modify all the exposed Tn antigen. Interestingly, *Maackia amurensis* hemagglutinin, a lectin that recognizes α2-3–linked sialic acid, stained *T-syn*$^{+/+}$ embryos much more strongly than *T-syn*$^{-/-}$ embryos (Fig. 4, A–D). This suggests that most α2-3–linked sialic acid is on core 1–derived O-glycans at this stage of development or that the lectin preferentially binds to α2-

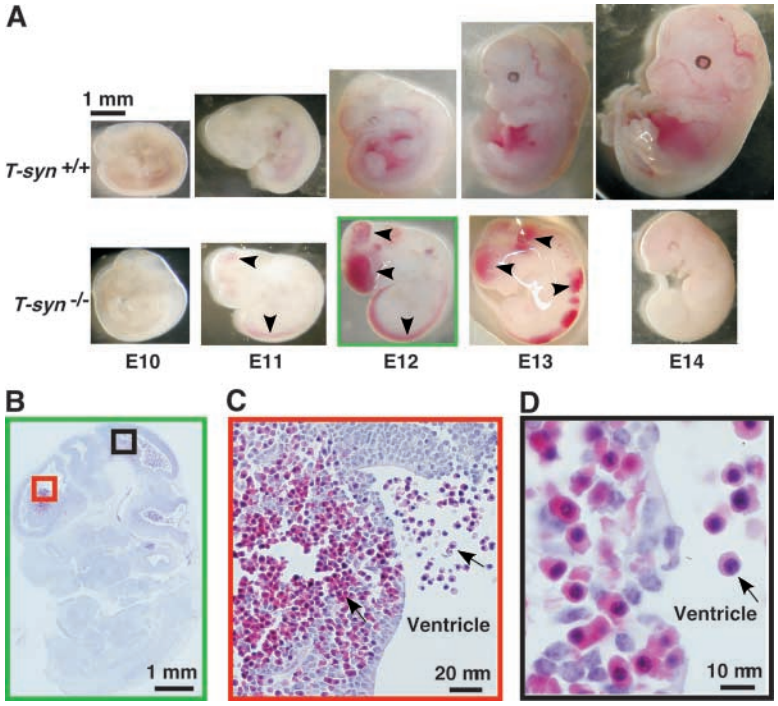

Figure 2. **Targeted disruption of *T-syn* causes fatal embryonic hemorrhage in mice.** (A) Comparison of *T-syn*$^{+/+}$ and *T-syn*$^{-/-}$ embryos at different developmental stages. Blood is visible in the hearts of the older *T-syn*$^{+/+}$ embryos. Arrowheads indicate hemorrhage in the brain parenchyma and ventricles, spinal cord, and spinal canal of *T-syn*$^{-/-}$ embryos. Less blood is detected in *T-syn*$^{-/-}$ hearts because of anemia. The E14 *T-syn*$^{-/-}$ embryo is dead and appears pale because blood circulation has ceased. (B) Sagittal section of the E12 *T-syn*$^{-/-}$ embryo. The red and black boxes indicate hemorrhagic lesions, which are shown at higher magnification in C and D. Bleeding is visible in both the brain parenchyma and ventricles. Arrows indicate erythrocytes, which are nucleated at this stage of development.

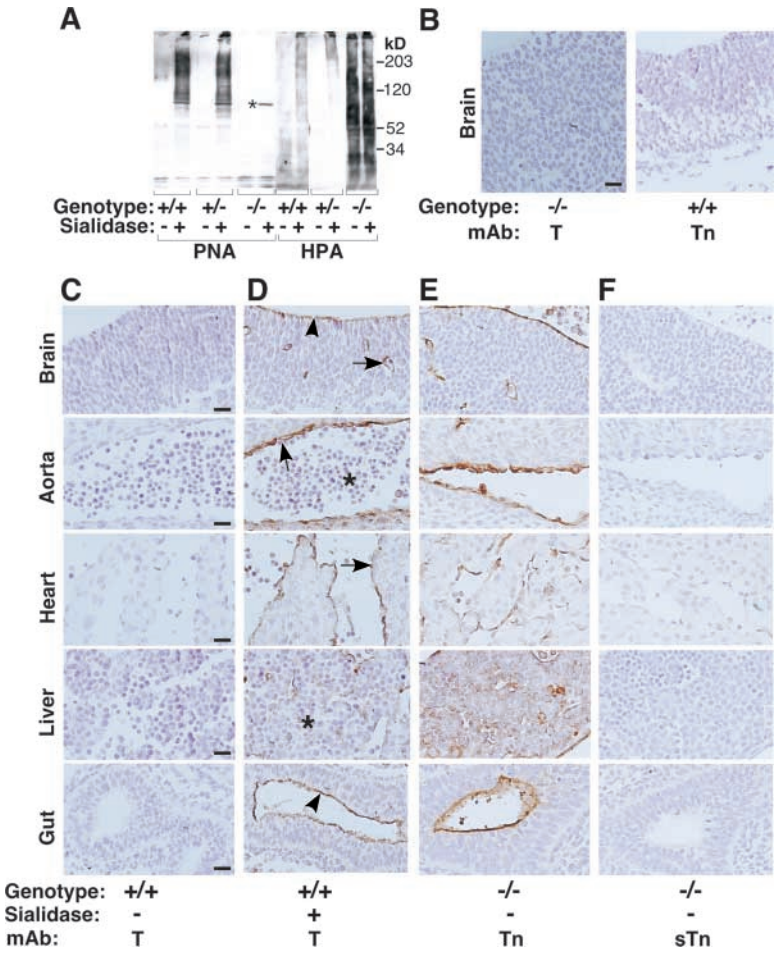

Figure 3. **Disruption of *T-syn* eliminates T antigen expression and exposes the Tn antigen in murine embryos.** (A) Blots of E12 tissue extracts probed with PNA, which recognizes nonsialylated core 1 O-glycans, and with HPA, which recognizes the nonsialylated Tn antigen. The extracts were incubated with or without sialidase before electrophoresis and blotting. The asterisk indicates the binding of PNA to the added sialidase. The blots are representative of three experiments. (B–F) Immunohistochemical staining of E12 tissue sections with mAbs to the T antigen, Tn antigen, or sialyl-Tn (sTn) antigen. The sections in D were pretreated with sialidase. Brown reaction product marks sites of antibody binding. Arrows, endothelial cells; arrowheads, epithelial cells; and asterisks, hematopoietic cells. Bars, 50 μm.

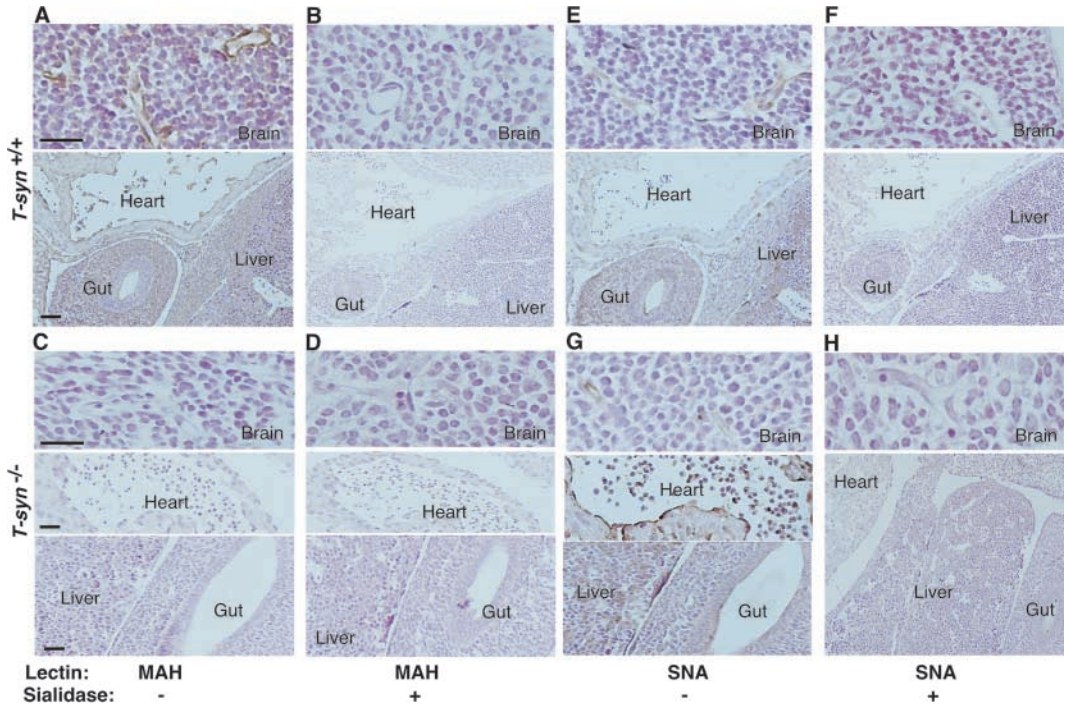

Figure 4. **Expression of α2-3–linked and α2-6–linked sialic acid in *T-syn*$^{+/+}$ and *T-syn*$^{-/-}$ embryos.** (A–H) Sections of the indicated tissues were pretreated with or without sialidase and stained with *Maackia amurensis* hemagglutinin (MAH), which recognizes α2-3–linked sialic acid, or with *Sambucus nigra* (SNA), which recognizes α2-6–linked sialic acid. Note that MAH binds much less to *T-syn*$^{-/-}$ embryos than to *T-syn*$^{+/+}$ embryos. Pretreatment of the sections with sialidase eliminated binding of MAH and SNA, confirming their specificity. Bars, 50 μm.

3–sialylated O-glycans. In contrast, *Sambucus nigra* agglutinin, which recognizes α2-6–linked sialic acid, stained *T-syn*$^{+/+}$ and *T-syn*$^{-/-}$ embryos equivalently (Fig. 4, E–H). Because *T-syn*$^{-/-}$ embryos add little or no α2-6–linked sialic acid to form the sialyl-Tn antigen, most of the α2-6–linked sialic acid may be on N-glycans.

T-syn$^{-/-}$ embryos have normal plasma-based blood coagulation

Hemorrhage may result from defects in the plasma or cellular components of the hemostatic system or in the vasculature. Some murine embryos lacking any one of several different coagulation proteins suffer fatal hemorrhage, but unlike *T-syn*$^{-/-}$ embryos, other embryos lacking the same protein escape bleeding and survive until birth (Bugge et al., 1996; Carmeliet et al., 1996; Connolly et al., 1996; Cui et al., 1996; Sun et al., 1998; Xue et al., 1998). Coagulation factors V and VIII are modified with O-glycans of unknown function (Kaufman, 1998). Plasma from *T-syn*$^{+/+}$ and *T-syn*$^{-/-}$ embryos clotted at similar rates as assessed by modified prothrombin times and activated partial thromboplastin times (Fig. 5, A and B). Furthermore, plasma from embryos of both genotypes corrected defective clotting of human plasma deficient in factor V or factor VIII (Fig. 5 C). These results argue against a general defect in plasma-based blood coagulation. O-glycosylation of platelet proteins might affect their hemostatic functions, but mice lacking platelets develop normally (Shivdasani et al., 1995). Because cell surface proteins rich in negatively charged, sialylated O-glycans have been suggested to reduce cell–cell interactions (Fukuda, 2002), we considered whether reduced sialylation of *T-syn*$^{-/-}$ blood cells might cause them to agglutinate and occlude vessels, leading to secondary hemorrhage. However, Wright-Giemsa–stained smears of *T-syn*$^{-/-}$ blood showed no agglutination. Intravital microscopy also revealed normal blood flow

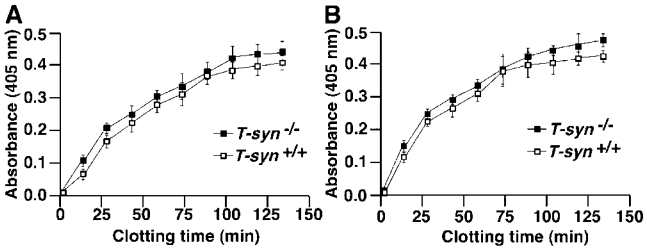

C

Supplement plasma	Coagulation time (sec) Factor V-deficient plasma	Factor VIII-deficient plasma
None	>500	153 ± 5
Normal human	125 ± 16	76 ± 2
E12 *T-syn* +/+	108 ± 25	55 ± 14
E12 *T-syn* -/-	131 ± 49	57 ± 16

Figure 5. **Plasma-based blood coagulation is equivalent in *T-syn*$^{+/+}$ and *T-syn*$^{-/-}$ embryos.** Clotting of individual plasma samples from eight E12 *T-syn*$^{+/+}$ embryos and six E12 *T-syn*$^{-/-}$ embryos (mean ± SD, $P > 0.05$) was measured by the kinetic activated partial thromboplastin time (A) and the kinetic prothrombin time (B). (C) The activated partial thromboplastin time of human plasma deficient in factor V or factor VIII was measured with or without supplementation with normal human plasma or with pooled plasma from *T-syn*$^{+/+}$ or *T-syn*$^{-/-}$ embryos. The data represent the mean ± SD of three independent experiments.

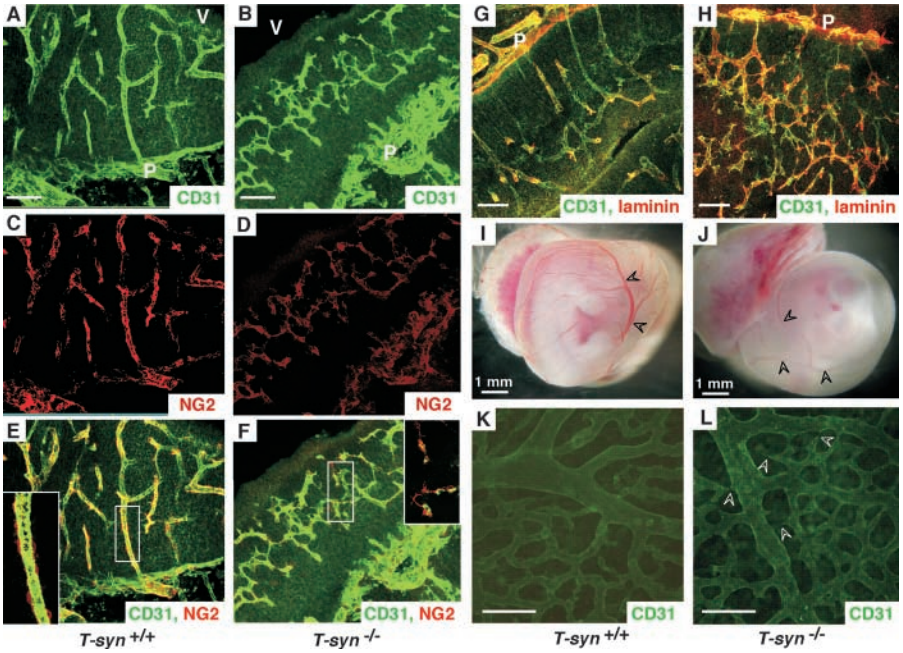

Figure 6. ***T-syn*$^{-/-}$ embryos develop a chaotic microvascular network.** (A–H) Visualization of microvessels in E12 hindbrains using maximal intensity projections of z-stacked confocal images. Endothelial cells were stained with antibodies to CD31 (green); pericytes were stained with antibodies to the proteoglycan NG2 (red); and basement membrane was stained with antibodies to laminin (red). *T-syn*$^{+/+}$ embryos form a network of capillaries with uniform diameters and a regular branching pattern (A, C, E, and G), whereas *T-syn*$^{-/-}$ embryos form capillaries with heterogeneous diameters and excessive, irregular branches (B, D, F, and H). Insets in E and F are thin (5 μm) optical slices of representative vessels enlarged 2.5-fold, which illustrate the abluminal relationship of the NG2-positive pericytes to the CD31-positive endothelial cells. P, perineural vascular plexus; V, ventricle. (I and J) The architecture of large vessels (arrowheads) is similar in *T-syn*$^{+/+}$ and *T-syn*$^{-/-}$ E12 yolk sacs, except that less blood fills the *T-syn*$^{-/-}$ vessels because of anemia. (K and L) Staining of whole mounts of E12 yolk sacs with antibodies to CD31. More capillary branching and irregular vessel diameters are present in the *T-syn*$^{-/-}$ yolk sac. Arrowheads indicate narrowed capillaries at branch points, which suggests incomplete vascular pruning. Bars, 50 μm, unless otherwise noted.

in large vessels of *T-syn*$^{-/-}$ yolk sacs, except that fewer cells circulated because of anemia (Videos 1 and 2, available at http://www.jcb.org/cgi/content/full/jcb.200311112/DC1).

T-syn$^{-/-}$ embryos develop a chaotic microvascular network

The earliest blood vessels arise by vasculogenesis, which is the differentiation of precursor cells into endothelial cells that form a primitive capillary plexus. New capillaries then develop by angiogenesis, in which endothelial cells migrate into previously avascular areas. These vessels mature as endothelial cells recruit pericytes, deposit extracellular matrix, and develop an organized branched network (Carmeliet, 2003; Jain, 2003). Mice lacking proteins that affect the recruitment or critical functions of endothelial cells or pericytes exhibit defective vasculogenesis or angiogenesis, and they frequently die from embryonic or perinatal hemorrhage (Liu et al., 2000; McCarty et al., 2002; Zhu et al., 2002; Carmeliet, 2003; Jain, 2003). Using confocal microscopy, we integrated optical slices of thick tissue sections to visualize the microvascular architectures of *T-syn*$^{+/+}$ and *T-syn*$^{-/-}$ E12 embryos. In brains of *T-syn*$^{+/+}$ embryos, endothelial cells marked by anti-CD31 antibodies were observed in the perineural plexus, which arises by vasculogenesis (Fig. 6 A). Endothelial cells in parenchymal vessels, which develop exclusively by angiogenesis, formed capillaries of relatively uniform diameters with orderly branching patterns. Pericytes marked by antibodies to the proteoglycan NG2 (Ozerdem et al., 2001) were associated with endothelial cells in both the perineural plexus and the brain parenchyma (Fig. 6, C and E). In brains of *T-syn*$^{-/-}$ embryos, endothelial cells and pericytes developed an apparently normal perineural plexus (Fig. 6, B, D, and F). However, endothelial cells in the brain parenchyma formed a chaotic microvasculature with irregular capillary diameters and disordered branching, indicating dysregulated angiogenesis (Fig. 6 B). Antibodies to NG2 stained the *T-syn*$^{-/-}$ brain vessel network, arguing that the vascular defect did not result from failure to recruit pericytes (Fig. 6, D and F). Laminin, a basement membrane component, was detected in the microvasculature of both *T-syn*$^{+/+}$ and *T-syn*$^{-/-}$ brains (Fig. 6, G and H). Confocal microscopy did not reveal obvious defects in the microvasculature of other *T-syn*$^{-/-}$ embryonic organs, and the architecture of large vessels in the yolk sac and other organs was grossly normal (Fig. 6, I and J). However, whole mounts demonstrated more capillary branching and more irregular vessel diameters in *T-syn*$^{-/-}$ yolk sacs than in *T-syn*$^{+/+}$ yolk sacs (Fig. 6, K and L). Immunoblots of *T-syn*$^{+/+}$ and *T-syn*$^{-/-}$ embryonic lysates showed no obvious differences in the levels of vascular endothelial growth factor, angiopoietin-1, Tie2, or platelet-derived growth factor B (unpublished data). This finding suggests that defective angiogenesis in *T-syn*$^{-/-}$ embryos does not result from a secondary increase or decrease in these known regulators of angiogenesis (Carmeliet, 2003; Jain, 2003).

T-syn$^{-/-}$ embryos have defective association of endothelial cells with pericytes and extracellular matrix

We used electron microscopy to better characterize the structures of *T-syn*$^{+/+}$ and *T-syn*$^{-/-}$ brain capillaries. The endothelial cells of *T-syn*$^{+/+}$ capillaries were relatively uniform in size and were intimately associated with pericytes (Fig. 7, A and E). In sharp contrast, most endothelial cells of *T-syn*$^{-/-}$ capillaries exhibited distorted shapes with irregular or dilated capillary lumens and with focal cytoplasmic thin-

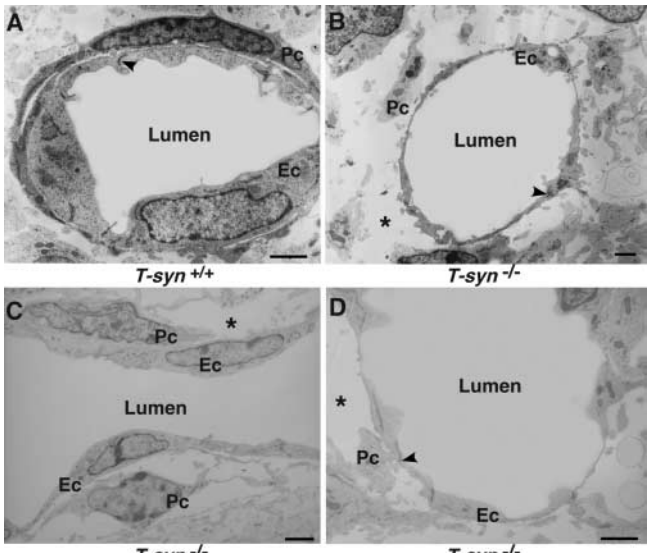

E

	EC w/ pericyte closely attached	EC w/o pericyte closely attached	Distorted EC	Total EC
T-syn $^{+/+}$	43	5	3	48
T-syn $^{-/-}$	7	30	33	37

Figure 7. ***T-syn*$^{-/-}$ embryos have defective capillary structures.** (A–D) Electron micrographs of sections from E12 brains. (A) A *T-syn*$^{+/+}$ capillary has a uniform lumen and a pericyte that is intimately associated with the endothelial cell. (B–D) *T-syn*$^{-/-}$ capillaries have distended or distorted lumens with attenuated endothelial cell processes. The upper pericyte in C is in close contact with an endothelial cell, but other pericytes are partially or completely separated from the endothelial cells. Large empty spaces (asterisks) surround the capillaries. Both *T-syn*$^{+/+}$ and *T-syn*$^{-/-}$ capillaries have normal interendothelial cell junctions (arrowheads). Ec, endothelial cell; Pc, pericyte. (E) Sections of capillaries were scored for pericytes closely attached to endothelial cells and for distortions in endothelial cell shape. Bars, 2 μm.

ning (Fig. 7, B–E). Mature interendothelial cell junctions were present, but pericytes typically lacked their normal close apposition to the endothelial cells. Many endothelial cells and pericytes were also surrounded by large spaces, indicating unstable interactions with the extracellular matrix or neighboring cells. The morphological abnormalities preceded hemorrhage and tended to be more severe near bleeding lesions. This implies that the structural defects are directly responsible for hemorrhage.

Discussion

Our results reveal a critical and unexpected contribution of core 1–derived O-glycans to angiogenesis. Blood vessels in the developing brain parenchyma arise exclusively by angiogenesis (Carmeliet, 2003; Jain, 2003), which probably explains why vascular defects in *T-syn*$^{-/-}$ embryos were most abundant in this tissue. The separation of endothelial cells from supporting pericytes and extracellular matrix is a likely mechanism for the capillary fragility in *T-syn*$^{-/-}$ embryos. The structural abnormalities might result from altered glycosylation of an adhesion molecule on cell surfaces or in the extracellular matrix, or they might develop through an O-glycosylation–dependent change in cell signaling. Endothelial cells and pericytes engage in bidirectional signaling that promotes vascular integrity and remodeling (Carmeliet, 2003; Jain, 2003). However, the vascular defects in *T-syn*$^{-/-}$ embryos do not appear to be due solely to defective support from pericytes. Mice lacking platelet-derived growth factor B or its receptor fail to recruit pericytes to developing brain vessels (Lindahl et al., 1997), yet they do not bleed until the late embryonic or perinatal period (Leveen et al., 1994; Soriano, 1994). In contrast, *T-syn*$^{-/-}$ embryos invariably die of hemorrhage by E14. This implies that one or more endothelial cell proteins require core 1–derived O-glycans to support angiogenesis. Targeted deletion of *T-syn* in endothelial cells will help address this possibility. The chaotic vascular branching in *T-syn*$^{-/-}$ embryonic brains indicates that the vessels fail to remodel into a hierarchical network.

The specific functions of core 1–derived O-glycans in angiogenesis remain to be determined. A core 1 O-glycan or one of its modified forms might serve as an essential ligand for an uncharacterized lectin. Myelin-associated glycoprotein (MAG), a member of the siglec family of lectins that recognize sialic acid–containing glycans (Crocker, 2002), binds exceptionally well to the sialyl-T antigen in vitro (Blixt et al., 2003). This raises the possibility that MAG, which is secreted from oligodendrocytes, might regulate angiogenesis by binding to the sialyl-T determinant on endothelial cell glycoproteins. However, MAG-deficient mice develop normally and do not have obvious defects in angiogenesis (Li et al., 1994). Therefore, defective interactions of MAG with sialylated core 1 O-glycans cannot be the sole explanation for the disordered angiogenesis in brains of *T-syn*$^{-/-}$ embryos. A core 1 O-glycan or one of its derivatives might also modulate the conformation of a protein that affects angiogenesis. Mucinlike domains have extended structures that are largely mediated by interactions of peptide-linked GalNAc residues with adjacent amino acids (Rose et al., 1984; Gerken et al., 1989; Shogren et al., 1989; Merry et al., 2003). The expression of the Tn antigen in *T-syn*$^{-/-}$ embryos suggests that these GalNAc–peptide interactions remain intact, which should prevent major structural changes in proteins that normally have many core 1–derived O-glycans. Defective core 1 O-glycosylation might still cause subtle, but functionally important, alterations in protein conformation or increase access to proteolytic attack. It is also possible that the exposed Tn antigen binds to an unknown lectin that interferes with angiogenesis.

Little is known about the synthesis of GalNAc-anchored O-glycans during development. A large family of *N*-acetylgalactosaminyltransferases transfer GalNAc from UDP-GalNAc to serine or threonine residues. During murine development, mRNAs encoding many of these enzymes are expressed in discrete patterns in multiple tissues, but their functions have not been addressed (Kingsley et al., 2000). Our immunohistochemical data indicate that core 1 O-glycans are expressed primarily in endothelial, hematopoietic, and epithelial cells during development. This suggests that these cells express the majority of the Ser/Thr-rich proteins that are O-glycosylated to become mucins. Other cells might express fewer or less clustered core 1 O-glycans that were not detected by immunohistochemistry. Most of the simple core 1 O-glycans (T antigen) were α2-3 sialylated to

form the sialyl-T antigen. Other core 1 O-glycans might be extended or branched to form more complex structures. The large reduction in binding of *Maackia amurensis* hemagglutinin to *T-syn*$^{-/-}$ embryonic tissues suggests that core 1–derived O-glycans display most of the α2-3–linked sialic acid. Although this decrease in sialylation could conceivably reduce charge-based repulsion among cells, we observed no evidence of abnormal cell agglutination in the circulation or in other tissues. This may be due to the continued expression of α2-6–linked sialic acid, which appeared to be present primarily on N-glycans. The Tn antigen exposed on endothelial, hematopoietic, and epithelial cells of *T-syn*$^{-/-}$ embryos was not α2-6 sialylated to form the sialyl-Tn antigen, as may occur on some malignant cells (Brockhausen et al., 1998).

Our data provide the first demonstration that normal development requires an O-glycosylation pathway that begins by attachment of GalNAc to serines or threonines. A much less common O-glycosylation pathway begins with direct attachment of fucose to serines or threonines on epidermal growth factor–like domains (Shao and Haltiwanger, 2003). Mice lacking the protein O-fucosyltransferase die in midgestation from multiple morphogenetic defects, reflecting the critical contribution of O-fucosylation to the Notch protein signaling pathway (Shi and Stanley, 2003). In contrast, defective angiogenesis leading to bleeding is the only detectable abnormality in *T-syn*$^{-/-}$ embryos. The relatively restricted expression of detectable core 1 O-glycans in endothelial, hematopoietic, and epithelial cells may explain why *T-syn*$^{-/-}$ embryos do not exhibit multiple developmental defects that cause earlier death. Core 1 O-glycans or their derivatives might contribute to physiological or pathological angiogenesis in adults. The expression of core 1 O-glycans in epithelial cells deserves further exploration, and other cells might express core 1 or core 2 O-glycans late in development or during adult life. Inducible or cell type–specific deletion of *T-syn* may reveal other important functions for core 1 O-glycosylation of proteins.

Materials and methods

Generation of *T-syn*$^{-/-}$ mice

All animal experiments were performed in compliance with relevant laws and were approved by the Institutional Animal Care and Use Committee of the Oklahoma Medical Research Foundation. A bacterial artificial chromosome containing the murine *T-syn* gene was identified by screening a murine embryonic stem cell library (Incyte Genomics) by PCR. Southern blot analysis showed that murine *T-syn*, like the corresponding human gene (Ju et al., 2002a), has three exons. Exon 1 is 0.3 kb and encodes the ATG translational start site, cytoplasmic domain, transmembrane domain, and stem region of T-synthase. Exon 2 is 0.6 kb and encodes the majority of the catalytic domain. Exon 3 is 0.3 kb and encodes the rest of the catalytic domain as well as the 3′-untranslated region. We engineered a targeting vector with three loxP sites in the *T-syn* allele, which flanked exons 1 and 2 and an inserted *Neo* cassette. The targeting vector was electroporated into CJ7 embryonic stem cells that were derived from a 129/SvImJ mouse (a gift from T. Sato, University of Texas Southwestern Medical School, Dallas, TX, with permission from T. Gridley, The Jackson Laboratory, Bar Harbor, ME). Embryonic stem cell clones with correct homologous recombination were screened by PCR and confirmed by Southern blots. Cells from one clone were transiently transfected with an expression vector encoding Cre recombinase (a gift from B. Sauer, Stowers Institute for Medical Research, Kansas City, MO) to delete exons 1 and 2 and the *Neo* cassette. Cells confirmed to have a normal karyotype were microinjected into C57BL/6J blastocysts, which were then implanted into pseudopregnant mice. Chimeras among the offspring were bred with C57BL/6J mice. Genotypes of mice were determined by PCR of DNA from tail biopsies or from portions of embryos or yolk sacs. The wild-type allele was identified using PCR 1 (primers 5′-TGGGTTATGACAAGTCCTC-3′ and 5′-TCATGTATCCCTGCTTCAC-3′). The mutant allele was detected by PCR 2 (primers 5′-GATAAATGTCTTACAGAAGG-3′ and 5′-AATACTGTCCTGGGCTATACTACAGTG-3′). Comparative studies of *T-syn*$^{+/+}$, *T-syn*$^{+/-}$, and *T-syn*$^{-/-}$ embryos were always performed with embryos from the same litter.

Glycosyltransferase assays

T-synthase activity from murine embryo extracts was measured using GalNAcα1-*O*-phenyl (Sigma-Aldrich) as an acceptor (Ju et al., 2002b). UDP-[^{3}H]Gal (40–60 Ci/mmol) was obtained from American Radiolabeled Chemicals, Inc. Activity of a control enzyme, β1-4-galactosyltransferase, was measured using GlcNAc-S-pNp (American Radiolabeled Chemicals, Inc.) as the acceptor in a 50-μl reaction containing 50 mM Tris-HCl, pH 7.0, 2 mM GlcNAc-S-pNp, 200 μM UDP-[^{3}H]Gal (60,000–90,000 cpm), 20 mM $MnCl_2$, 0.1% Triton X-100, and 100 μg of protein from embryo extracts. The reactions were incubated at 37°C for 1 h and stopped by adding 950 μl of cold H_2O. The products were separated from UDP-[^{3}H]Gal by Sep-Pak (C18; Waters Corporation) column chromatography and were quantified (Ju et al., 2002b).

Lectin blots and immunoblots

Embryo extracts (40 μg of protein) with or without prior desialylation were resolved by SDS-PAGE under reducing conditions and transferred to a nitrocellulose membrane (Bio-Rad Laboratories). For desialylation, 200 μg of embryonic protein in a 40-μl reaction volume was incubated with 20 mU sialidase from *Arthrobacter ureafaciens* (Roche) overnight at 37°C. The membrane was blocked with 5% nonfat dry milk and incubated with 2 μg/ml HRP-conjugated PNA or 0.25 μg/ml HPA (EY Laboratories) in TBS at RT for 1 h. Lectin binding was detected with chemiluminescent substrate (HighSignal West Pico; Pierce Chemical Co.). Alternatively, the membrane was probed with rabbit antibodies to angiopoetin 1, Tie2, VEGF, PDGF B, and actin (Santa Cruz Biotechnology, Inc.). Binding was detected with HRP-conjugated goat anti–rabbit IgG (Pierce Chemical Co.) using ECL (Amersham Biosciences).

Blood coagulation assays

2–3 μl of blood from E12 embryos was harvested into 40 μl TBS containing 0.19% sodium citrate. Plasma was obtained after centrifugation. Kinetic coagulation assays in 96-well microtiter plates were conducted using minor modifications of protocols described for zebrafish (Sheehan et al., 2001). In brief, 10 μl of plasma from each embryo, adjusted to the same protein concentration, was added to a well containing 3 mg/ml of purified human fibrinogen (Calbiochem) in a total volume of 50 μl. For the kinetic activated partial thromboplastin time, 15 μl of partial thromboplastin reagent (Dade Actin; Dade Behring, Inc.) and 8 mM $CaCl_2$ were added. For the kinetic prothrombin time, 30 μl Thromboplastina C Plus (Dade Behring, Inc.) was added. Clot formation at RT was monitored with a kinetic microplate reader (Molecular Devices) set at 405 nm. Embryo plasma was replaced with TBS as a negative control.

For the coagulation correction assay, 50 μl of pooled murine embryo plasma was mixed with 100 μl of human plasma deficient in factor V or factor VIII (Fisher Scientific). Coagulation triggered by the addition of partial thromboplastin reagent and $CaCl_2$ was measured on a coagulation analyzer (model Start 4; Diagnostica Stago). Pooled normal human plasma diluted to the same protein concentration as the embryo plasma was used as a positive control.

Microscopy

Embryos were photographed at autopsy. For routine histological analysis, embryos were fixed in 10% neutral pH formalin overnight at 4°C, embedded in paraffin, sectioned at 4-μm thickness, and stained with hematoxylin-eosin. For immunohistochemistry, deparaffinized sections were incubated with or without 0.5 U/ml sialidase from *Arthrobacter ureafaciens* at 37°C for 3 h. Sections were incubated with mAbs against the T, Tn, or sialyl-Tn antigens (Mandel et al., 1991; mouse IgG or IgM, gifts from U. Mandel and H. Clausen, School of Dentistry, University of Copenhagen, Copenhagen, Denmark) or with isotype-matched control mouse IgG or IgM. Bound antibodies were detected with HRP-conjugated goat anti–mouse IgG/IgM (DakoCytomation). Alternatively, sections were incubated with peroxidase-conjugated *Maackia amurensis* or *Sambucus nigra* hemagglutinin (EY Laboratories). Immunohistochemical staining was developed with a DAB peroxidase substrate kit (Vector Laboratories).

For confocal microscopy, embryos were fixed in 4% PFA in 0.1 M PBS at RT for 90–120 min, washed, cryoprotected with 15% sucrose in PBS at

4°C overnight, mounted in Tissue-Tek O.C.T. compound, and snap-frozen in liquid nitrogen–cooled isopentane. 100-μm-thick cryosections were quenched with 0.1 M glycine in PBS, washed twice, and blocked with 3% BSA in PBS containing 0.01% saponin. Sections were incubated with rat anti–murine CD31 mAb (1:10 dilution; BD Biosciences) and rabbit anti-NG2 antibody (1:200 dilution; Chemicon) in 0.3% BSA in PBS with 0.01% saponin or with rabbit antilaminin antibody (1:500 dilution; DakoCytomation) for 1 h at RT. Thereafter, the sections were washed in PBS containing 0.01% saponin and incubated with Cy3-conjugated goat anti–rabbit antibody (1:100 dilution; Vector Laboratories) and biotinylated goat anti–rat IgG absorbed to remove anti–murine IgG (1:100 dilution; Vector Laboratories), followed by streptavidin conjugated to FITC (1:100 dilution; Vector Laboratories). The sections were mounted with Vectashield (Vector Laboratories) and analyzed by three-dimensional confocal laser scanning microscopy using a scanning head (model C1; Nikon) mounted on an inverted microscope (model ECLIPSE 2000U; Plan Apochromats dry objective lens, 20×, NA 0.75; Nikon). Z-stack images were collected at 1-μm steps with sequential laser excitation to eliminate bleedthrough and with confocal parameters selected to minimize the thickness of the calculated optical section. Volume images from the confocal data sets were processed with IMARIS software (Bitplane AG) for three-dimensional views of the detailed vascular morphology. Images are presented as maximum intensity projections of the z stacks.

For whole-mount immunofluorescence, yolk sacs were fixed in 4% PFA in 0.1 M PBS at RT for 60 min and incubated sequentially with rat anti–mouse CD31 mAb, biotinylated goat anti–rat IgG, and streptavidin conjugated to FITC. The yolk sacs were mounted on slides and visualized with a Micro and Macro instrument (model ECLIPSE E800M; Nikon).

For transmission electron microscopy, embryos were fixed with 3% PFA and 2% glutaraldehyde in 0.1 M cacodylate, pH 7.2, for 2 h, postfixed in 2% osmium tetroxide in 0.1 M cacodylate, dehydrated in acetone series, and embedded in EMbed 812 epoxy resin (Electron Microscopy Sciences, Inc.). Thin sections stained with uranyl acetate and lead citrate were examined with an electron microscope (model JEM-1200EX; Jeol).

Intravital microscopy of embryos was performed using procedures described previously for adult mice (Xia et al., 2002).

Online supplemental material

Video microscopy of yolk sac blood vessels from living E12 *T-syn*$^{+/+}$ embryos (Video 1, wild type) and *T-syn*$^{-/-}$ embryos (Video 2, T-syn deficient). Blood flow is normal in both yolk sacs, except that fewer blood cells are seen in the *T-syn*$^{-/-}$ vessels because of anemia. Online supplemental material is available at http://www.jcb.org/cgi/content/full/jcb.200311112/DC1.

We thank Christer Betsholtz and Thomas Sato for insightful suggestions and critical reading of the manuscript and Charles Esmon and Ute Hochgeschwender for advice on experimental protocols. Microinjection of blastocysts was performed by Margaret Ober and Rowena Crittenden at the University of Virginia microinjection facility, directed by Sonia Pearson-White. We thank Todd Walker for computer support and Ulla Mandel, Henrik Clausen, and Thomas Sato for providing reagents.

This work was supported by National Institutes of Health (NIH) grants HL 54502 (to R.P. McEver), AI 48075 (to R.D. Cummings), and RR 018758 (to R.P. McEver, L. Xia, and R.D. Cummings), and by a Scientist Development Grant from the American Heart Association (to L. Xia). Tissue processing and electron microscopy were performed in the imaging core facility of the Oklahoma Medical Research Foundation, supported in part by NIH grant RR 15577.

Submitted: 21 November 2003
Accepted: 23 December 2003

References

Berger, E.G. 1999. Tn-syndrome. *Biochim. Biophys. Acta.* 1455:255–268.

Blixt, O., B.E. Collins, I.M. Van Den Nieuwenhof, P.R. Crocker, and J.C. Paulson. 2003. Sialoside specificity of the siglec family assessed using novel multivalent probes: identification of potent inhibitors of myelin-associated glycoprotein. *J. Biol. Chem.* 278:31007–31019.

Brockhausen, I. 1999. Pathways of O-glycan biosynthesis in cancer cells. *Biochim. Biophys. Acta.* 1473:67–95.

Brockhausen, I., J. Yang, N. Dickinson, S. Ogata, and S.H. Itzkowitz. 1998. Enzymatic basis for sialyl-Tn expression in human colon cancer cells. *Glycoconj. J.* 15:595–603.

Bugge, T.H., Q. Xiao, K.W. Kombrinck, M.J. Flick, K. Holmback, M.J. Danton, M.C. Colbert, D.P. Witte, K. Fujikawa, E.W. Davie, and J.L. Degen. 1996. Fatal embryonic bleeding events in mice lacking tissue factor, the cell-associated initiator of blood coagulation. *Proc. Natl. Acad. Sci. USA.* 93:6258–6263.

Carmeliet, P. 2003. Angiogenesis in health and disease. *Nat. Med.* 9:653–660.

Carmeliet, P., N. Mackman, L. Moons, T. Luther, P. Gressens, I. Van Vlaenderen, H. Demunck, M. Kasper, G. Breier, P. Evrard, et al. 1996. Role of tissue factor in embryonic blood vessel development. *Nature.* 383:73–75.

Connolly, A.J., H. Ishihara, M.L. Kahn, R.V. Farese, Jr., and S.R. Coughlin. 1996. Role of the thrombin receptor in development and evidence for a second receptor. *Nature.* 381:516–519.

Crocker, P.R. 2002. Siglecs: sialic-acid-binding immunoglobulin-like lectins in cell-cell interactions and signalling. *Curr. Opin. Struct. Biol.* 12:609–615.

Cui, J., K.S. O'Shea, A. Purkayastha, T.L. Saunders, and D. Ginsburg. 1996. Fatal haemorrhage and incomplete block to embryogenesis in mice lacking coagulation factor V. *Nature.* 384:66–68.

Daniels, M.A., L. Devine, J.D. Miller, J.M. Moser, A.E. Lukacher, J.D. Altman, P. Kavathas, K.A. Hogquist, and S.C. Jameson. 2001. CD8 binding to MHC class I molecules is influenced by T cell maturation and glycosylation. *Immunity.* 15:1051–1061.

Fukuda, M. 2002. Roles of mucin-type O-glycans in cell adhesion. *Biochim. Biophys. Acta.* 1573:394–405.

Gerken, T.A., K.J. Butenhof, and R. Shogren. 1989. Effects of glycosylation on the conformation and dynamics of O-linked glycoproteins: carbon-13 NMR studies of ovine submaxillary mucin. *Biochemistry.* 28:5536–5543.

Jain, R.K. 2003. Molecular regulation of vessel maturation. *Nat. Med.* 9:685–693.

Ju, T., and R.D. Cummings. 2002. A unique molecular chaperone Cosmc required for activity of the mammalian core 1 beta 3-galactosyltransferase. *Proc. Natl. Acad. Sci. USA.* 99:16613–16618.

Ju, T., K. Brewer, A. D'Souza, R.D. Cummings, and W.M. Canfield. 2002a. Cloning and expression of human core 1 beta1,3-galactosyltransferase. *J. Biol. Chem.* 277:178–186.

Ju, T., R.D. Cummings, and W.M. Canfield. 2002b. Purification, characterization, and subunit structure of rat core 1 Beta1,3-galactosyltransferase. *J. Biol. Chem.* 277:169–177.

Kaufman, R.J. 1998. Post-translational modifications required for coagulation factor secretion and function. *Thromb. Haemost.* 79:1068–1079.

Kingsley, P.D., K.G. Hagen, K.M. Maltby, J. Zara, and L.A. Tabak. 2000. Diverse spatial expression patterns of UDP-GalNAc:polypeptide N-acetylgalactosaminyl-transferase family member mRNAs during mouse development. *Glycobiology.* 10:1317–1323.

Kudo, T., T. Iwai, T. Kubota, H. Iwasaki, Y. Takayma, T. Hiruma, N. Inaba, Y. Zhang, M. Gotoh, A. Togayachi, and H. Narimatsu. 2002. Molecular cloning and characterization of a novel UDP-Gal:GalNAc(alpha) peptide beta 1,3-galactosyltransferase (C1Gal-T2), an enzyme synthesizing a core 1 structure of O-glycan. *J. Biol. Chem.* 277:47724–47731.

Leveen, P., M. Pekny, S. Gebre-Medhin, B. Swolin, E. Larsson, and C. Betsholtz. 1994. Mice deficient for PDGF B show renal, cardiovascular, and hematological abnormalities. *Genes Dev.* 8:1875–1887.

Li, C., M.B. Tropak, R. Gerlai, S. Clapoff, W. Abramow-Newerly, B. Trapp, A. Peterson, and J. Roder. 1994. Myelination in the absence of myelin-associated glycoprotein. *Nature.* 369:747–750.

Lindahl, P., B.R. Johansson, P. Leveen, and C. Betsholtz. 1997. Pericyte loss and microaneurysm formation in PDGF-B-deficient mice. *Science.* 277:242–245.

Liu, Y., R. Wada, T. Yamashita, Y. Mi, C.X. Deng, J.P. Hobson, H.M. Rosenfeldt, V.E. Nava, S.S. Chae, M.J. Lee, et al. 2000. Edg-1, the G protein-coupled receptor for sphingosine-1-phosphate, is essential for vascular maturation. *J. Clin. Invest.* 106:951–961.

Lowe, J.B., and J.D. Marth. 2003. A genetic approach to mammalian glycan function. *Annu. Rev. Biochem.* 72:643–691.

Mandel, U., O.W. Petersen, H. Sorensen, P. Vedtofte, S. Hakomori, H. Clausen, and E. Dabelsteen. 1991. Simple mucin-type carbohydrates in oral stratified squamous and salivary gland epithelia. *J. Invest. Dermatol.* 97:713–721.

McCarty, J.H., R.A. Monahan-Earley, L.F. Brown, M. Keller, H. Gerhardt, K. Rubin, M. Shani, H.F. Dvorak, H. Wolburg, B.L. Bader, et al. 2002. Defective associations between blood vessels and brain parenchyma lead to cerebral hemorrhage in mice lacking alphav integrins. *Mol. Cell. Biol.* 22:7667–7677.

McEver, R.P. 2002. Selectins: lectins that initiate cell adhesion under flow. *Curr. Opin. Cell Biol.* 14:581–586.

Merry, A.H., R.J. Gilbert, D.A. Shore, L. Royle, O. Miroshnychenko, M. Vuong, M.R. Wormald, D.J. Harvey, R.A. Dwek, B.J. Classon, et al. 2003. O-glycan sialylation and the structure of the stalk-like region of the T cell coreceptor CD8. *J. Biol. Chem.* 278:27119–27128.

Moody, A.M., D. Chui, P.A. Reche, J.J. Priatel, J.D. Marth, and E.L. Reinherz. 2001. Developmentally regulated glycosylation of the CD8alphabeta coreceptor stalk modulates ligand binding. *Cell.* 107:501–512.

Moody, A.M., S.J. North, B. Reinhold, S.J. Van Dyken, M.E. Rogers, M. Panico, A. Dell, H.R. Morris, J.D. Marth, and E.L. Reinherz. 2003. Sialic acid capping of CD8beta core 1-O-glycans controls thymocyte-major histocompatibility complex class I interaction. *J. Biol. Chem.* 278:7240–7246.

Ozerdem, U., K.A. Grako, K. Dahlin-Huppe, E. Monosov, and W.B. Stallcup. 2001. NG2 proteoglycan is expressed exclusively by mural cells during vascular morphogenesis. *Dev. Dyn.* 222:218–227.

Rose, M.C., W.A. Voter, H. Sage, C.F. Brown, and B. Kaufman. 1984. Effects of deglycosylation on the architecture of ovine submaxillary mucin glycoprotein. *J. Biol. Chem.* 259:3167–3172.

Shao, L., and R.S. Haltiwanger. 2003. O-fucose modifications of epidermal growth factor-like repeats and thrombospondin type 1 repeats: unusual modifications in unusual places. *Cell. Mol. Life Sci.* 60:241–250.

Sheehan, J., M. Templer, M. Gregory, R. Hanumanthaiah, D. Troyer, T. Phan, B. Thankavel, and P. Jagadeeswaran. 2001. Demonstration of the extrinsic coagulation pathway in teleostei: identification of zebrafish coagulation factor VII. *Proc. Natl. Acad. Sci. USA.* 98:8768–8773.

Shi, S., and P. Stanley. 2003. Protein O-fucosyltransferase 1 is an essential component of Notch signaling pathways. *Proc. Natl. Acad. Sci. USA.* 100:5234–5239.

Shivdasani, R.A., M.F. Rosenblatt, D. Zucker-Franklin, C.W. Jackson, P. Hunt, C.J. Saris, and S.H. Orkin. 1995. Transcription factor NF-E2 is required for platelet formation independent of the actions of thrombopoietin/MGDF in megakaryocyte development. *Cell.* 81:695–704.

Shogren, R., T.A. Gerken, and N. Jentoft. 1989. Role of glycosylation on the conformation and chain dimensions of O-linked glycoproteins: light-scattering studies of ovine submaxillary mucin. *Biochemistry.* 28:5525–5536.

Soriano, P. 1994. Abnormal kidney development and hematological disorders in PDGF beta-receptor mutant mice. *Genes Dev.* 8:1888–1896.

Sun, W.Y., D.P. Witte, J.L. Degen, M.C. Colbert, M.C. Burkart, K. Holmback, Q. Xiao, T.H. Bugge, and S.J. Degen. 1998. Prothrombin deficiency results in embryonic and neonatal lethality in mice. *Proc. Natl. Acad. Sci. USA.* 95: 7597–7602.

Van den Steen, P., P.M. Rudd, R.A. Dwek, and G. Opdenakker. 1998. Concepts and principles of O-linked glycosylation. *Crit. Rev. Biochem. Mol. Biol.* 33: 151–208.

Van Zante, A., and S.D. Rosen. 2003. Sulphated endothelial ligands for L-selectin in lymphocyte homing and inflammation. *Biochem. Soc. Trans.* 31:313–317.

Xia, L., M. Sperandio, T. Yago, J.M. McDaniel, R.D. Cummings, S. Pearson-White, K. Ley, and R.P. McEver. 2002. P-selectin glycoprotein ligand-1-deficient mice have impaired leukocyte tethering to E-selectin under flow. *J. Clin. Invest.* 109:939–950.

Xue, J., Q. Wu, L.A. Westfield, E.A. Tuley, D. Lu, Q. Zhang, K. Shim, X. Zheng, and J.E. Sadler. 1998. Incomplete embryonic lethality and fatal neonatal hemorrhage caused by prothrombin deficiency in mice. *Proc. Natl. Acad. Sci. USA.* 95:7603–7607.

Zhu, J., K. Motejlek, D. Wang, K. Zang, A. Schmidt, and L.F. Reichardt. 2002. beta8 integrins are required for vascular morphogenesis in mouse embryos. *Development.* 129:2891–2903.